Int. J. Environ. Sci. Technol. (2015) 12:3489–3498
DOI 10.1007/s13762-015-0882-2

ORIGINAL PAPER

Decomposition of gas-phase chloroform using nanophotocatalyst downstream the novel non-thermal plasma reactor: by-products elimination

F. Ghorbani Shahna[1] · **H. Ebrahimi**[1] · **B. Jaleh**[2] · **A. Bahrami**[1]

Received: 26 October 2014 / Revised: 5 May 2015 / Accepted: 22 August 2015 / Published online: 7 September 2015

Abstract Combination the non-thermal plasma technique by photocatalytic oxidation can enhance volatile organic compounds degradation. In this study, the decomposition of chloroform vapors in a novel non-thermal plasma reactor as well as an integrated system of this reactor in conjunction with the photocatalysis process was investigated. Expanded graphite was used as discharge electrode of dielectric barrier discharge reactor and the support of TiO_2 and ZnO catalysts as well. Results showed that chloroform degradation increased in hybrid system. The non-thermal plasma reactor had high content of NO and NO_2, whereas the concentration of these two pollutants dropped dramatically in hybrid system; moreover, the generated ozone from the non-thermal plasma process was degraded on the photocatalyst and consequently was not detected in the output gas of the combined system. The generated organic by-products in non-thermal plasma process (phosgene and trichloroacetaldehyde) were reoxidized with un-oxidized chloroform in the second stage of the combined system. This increased the selectivity of CO_2 and Cl_2.

Keywords Non-thermal plasma · Photocatalytic oxidation · Chloroform · Expanded graphite

Introduction

In the last 20 years, biologic process, photocatalysis process and plasma technology have been considered as methods for removal of volatile organic compounds (VOCs) and chlorinated volatile organic compounds (CVOCs) (Subrahmanyam et al. 2007a, b; Zhu et al. 2008). Non-thermal (non-equilibrium) plasma (NTP) has been more taken into account for VOCs degradation because it creates a very strong radical and oxidant agents degrading VOC molecules in ambient pressure and temperature (Magureanu et al. 2007). Plasma reactors have been constructed in various designs and models. Dielectric barrier discharge (DBD) reactor is one of the reactors used in NTP technology. Dielectric barrier leads to the creation of micro-discharge that is distributed in the total space and volume of the reactor (Subrahmanyam et al. 2007a, b).

Application of the NTP technique is limited due to the formation of harmful by-products such as carbon monoxide, ozone and NO_x (Subrahmanyam et al. 2007a, b). The efficiency of the NTP technique can be raised by two factors: (1) eliminating unwanted by-products; (2) reduction in energy consumption. It seems that increasing the residence time of pollutants in plasma reactor without changing the size of the reactor and transferring the by-products toward reoxidation are appropriate options for increasing efficiency (Subrahmanyam et al. 2006). In recent years, many researchers have investigated the combination of NTP with photocatalytic oxidation (PCO); they have reported that this system has a synergistic effect (Huang and Ye 2009; Lu et al. 2012; Maciuca et al. 2012; Sun et al. 2007; Thevenet et al. 2007; Zhu et al. 2008). In this system, the activation of catalyst is attributed to the light emitted and active species created by the plasma. Furthermore, the created ozone and chlorine radicals

---

✉ H. Ebrahimi
Hossein.ebrahimi@yahoo.com

[1] Center of excellence for occupational health, Research center for health science, School of Public Health, Hamadan University of Medical Sciences, Hamadan, Iran

[2] Faculty of Physics, Bu-Ali Sina University, Hamadan, Iran

(chlorinated compounds) by plasma can also activate the deactivated sites of the catalyst. In combined system, in addition to processes of plasma and PCO, because of the generated ozone, catalytic ozonation and ozone photolysis (UV/O_3) also contribute to pollutant degradation. This increase of oxidation process leads to an increase in oxidation agents: hydroxyl, proxy and so forth, which as a whole results in a synergistic effect on organic compounds removal. In this system, the unoxidized pollutant and generated by-products resulted from the plasma process (organic by-products, CO, NO_x and ozone) are reoxidized by the mentioned methods which cause an increase in removal efficiency of the pollutant and selectivity of CO_2 (Huang and Ye 2009; Lu et al. 2012).

The objective of this study was to investigate the effect of the combined system of PCO with NTP on the removal of chloroform vapors. For this reason, the effects of plasma discharge electrode, the applied voltage, the inlet concentration and flow rate on the chloroform removal were studied. Furthermore, the effects of this system on the elimination of by-products such as phosgene, trichloroacetaldehyde, ozone and NO_x were investigated. The research was conducted from November 2013 to April 2014 in the laboratory of Hamedan University of Medical Sciences.

Materials and methods

Experimental detail

The experimental setup has been illustrated in Fig. 1. The chloroform vapors (85, 250 and 500 ppm in air) was introduced into the reactor with flow rates of 0.3, 0.6 and 1.2 L/min corresponding to gas residence times of 2, 1 and 0.5 s, respectively. The concentration of chloroform was measured by a gas chromatograph (GC-2010, Shimadzu, Japan) equipped with a hydrogen flame ionization detector (FID) and 25 m long SGE capillary column (fused silica, film thickness: 0.25 micron, ID: 0.22 mm). In addition to this, a gas chromatograph/mass spectrometer (Varian, CP-3800, USA) was used to identify by-products. The ozone and NO_x concentrations were measured by an ozone monitor (EST 1015, USA) and a NO_x analyzer (G 750 polytector2), respectively. The experiments were repeated twice.

The DBD reactor was rectangular cube in shape, with quartz walls of 2 mm thickness, 150 mm length, 20 mm height and 10 mm width (Fig. 2). The novelty of the DBD reactor was that the expanded graphite (EG) acted as the discharge electrode. The discharge gap was fixed at 15 mm and discharge length was 50 mm. A copper plate with a

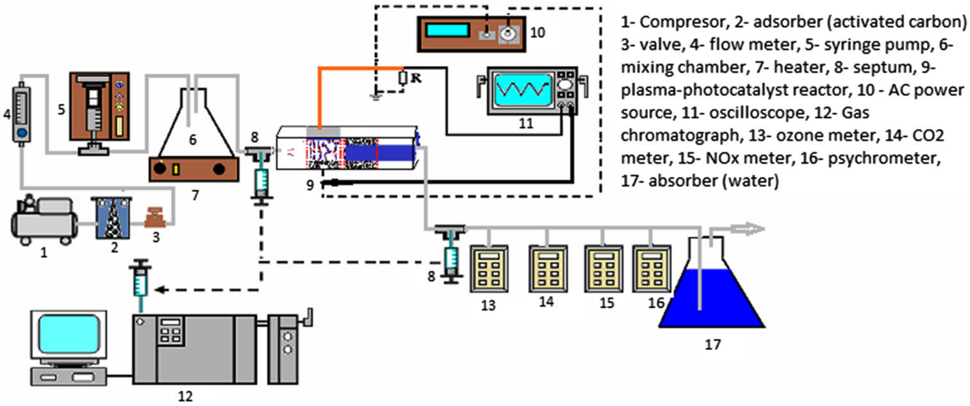

Fig. 1 A schematic diagram of the experimental setup

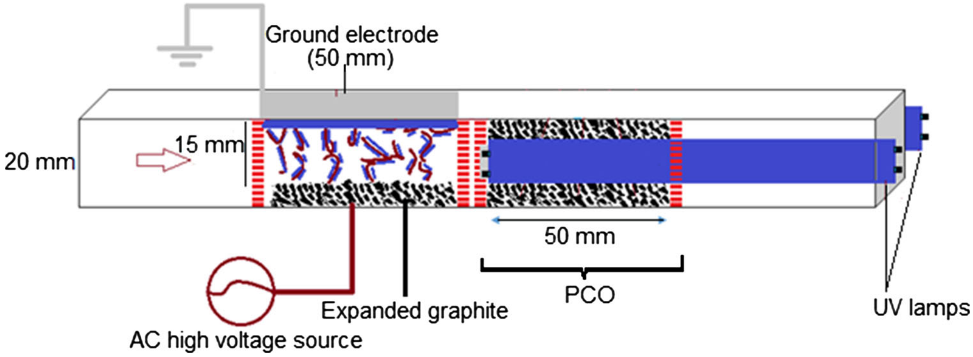

Fig. 2 Schematic overview of DBD–PCO reactor

length of 50 mm on the top of the reactor acted as the ground electrode. The EG was connected to a high-voltage alternating current (AC) (0–30 kV, 52–30,000 Hz) through a high-voltage wire. Electrical parameters were monitored by an oscilloscope (Oscilloscope Hameg HM-203-720 MHz Dual Trace, UK) that was connected to the DBD reactor through a high-voltage probe (1000–1). The applied voltages were 15 and 20 kV.

In order to combine photocatalyst with NTP, EG was replaced with EG-TiO_2&ZnO nanocomposite; the EG-TiO_2&ZnO nanocomposite acted as the discharge electrode. The EG-TiO_2&ZnO nanocomposite did not act as the discharge electrode in applied voltages, due to changes in the electrical properties of EG because of TiO_2 and ZnO coating. Therefore, downstream NTP, the reactor was filled with EG-TiO_2&ZnO nanocomposite (length of 50 mm). UV radiation was provided by two black light lamps with wavelength of 253.7 nm (Philips TUV 8 W/G8 T5 Bulb) placed the sides of the reactor (Fig. 2). In order to avoid interference from ambient lighting, the reactor was placed inside a dark chamber.

Synthesis of EG and EG-TiO_2&ZnO nanocomposite

By using the thermal shock method, in the range of 1000–1050 °C for 30 s, the expandable graphite (Beijing invention biology engineering and new materials, China) was converted to the EG.

The EG-TiO_2&ZnO nanocomposite was prepared on the base of the sol–gel method. Initially, the TiO_2 and ZnO sols were made. TiO_2 sol was made by using titanium-n-butoxide as the precursor. 2.04 mL Ti (OBu) 4 diluted with 36.64 mL PrOH as solvent, and the resultant mixture was stirred at room temperature for 1 h. Acetyl acetone was added dropwise to the mixed solution under a stirring as stabilizer, and then, the solution was stirred for 2 h. Next, the HNO_3 aqueous solution was added under stirring ensuring a pH of the sol–gel solution of about 2. Finally, the solution was refluxed for 8 h to obtain crystalline anatase sol (Yan and Chunwei 2006). To prepare ZnO sol, 8.76 g zinc acetate dehydrate in 200 mL of ethanol in a water bath (50° C) under stirring with a magnetic stirrer was solved. Then, 5.96 g of triethanolamine was added to the solution. After one hour, the solution was removed and ultrasonically treated for 30 min at 40° C (Pal and Sharon 2002). These sols were combined in equal amounts; then, the EG was added to the combined sol and placed in a dark location for 2 days; next, the smooth and dried samples were placed in a furnace with temperature of 400° C for 2 h for calcination. The synthesized EG-TiO_2&ZnO nanocomposite was characterized by SEM (TESCAN, MIRA3, USA) and XRD (APD 2000 XRD, Italy) techniques.

Results and discussion

Characteristics of EG-TiO_2&ZnO nanocomposite

XRD analysis was carried out over the 2θ range of 2–90° for the EG-TiO_2&ZnO nanocomposite. Figure 3 shows the XRD patterns of the EG-TiO_2&ZnO nanocomposite after heat treatment at 400° C for 2 h. Major peaks for TiO_2 nanoparticles were detected at 2θs of 25.2°, 38.5°, 53.8°,

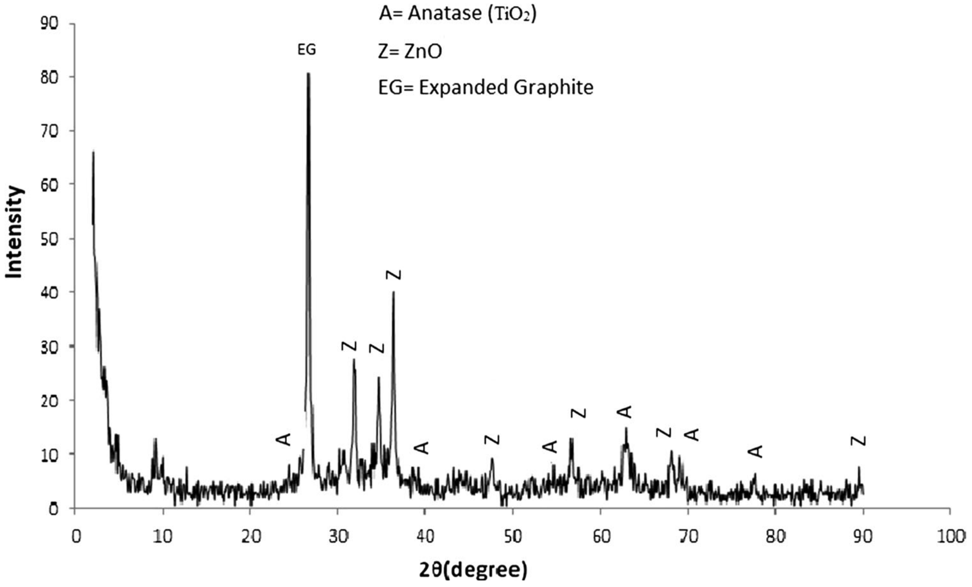

Fig. 3 XRD patterns of the EG-TiO_2&ZnO nanocomposite

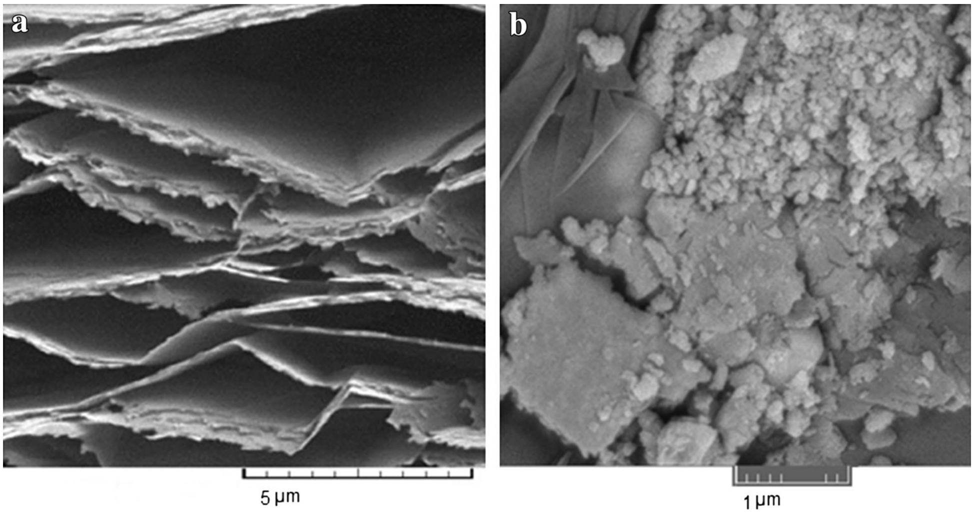

Fig. 4 SEM micrographs: **a** bare EG, **b** EG-TiO_2&ZnO nanocomposite

62.6°, 68.7° and 76.0°. They were assigned 101, 112, 105, 204, 116 and 301 diffraction peaks of the anatase TiO_2 (JCPDS No. 21-1272). And, for ZnO samples, major peaks were detected at 2θs of 31.7°, 34.4°, 36.2°, 47.5°, 56.6°, 67.9° and 89.6°. They were assigned 100, 002, 101, 102, 110, 112 and 203 diffraction peaks of the ZnO (JCPDS No. 70-2551).

SEM observations confirmed the results of the XRD analysis. It was found that both TiO_2 and ZnO particles had been coated on the surface of EG. Figure 4 represents the SEM images of both bare EG (a) and EG, which was loaded by TiO_2 and ZnO (b). It is clearly seen that the EG had a porous structure, and spacing of the interlayers of EG flakes was high (Fig. 4a).

The differences in morphology could be clearly observed by comparing Fig. 4a and b. After coating and calcination, it was clearly seen that the EG structure had changed and broken up to small fragments. Moreover, it was found that the TiO_2 and ZnO particles had a nanosize and were well spread on the surface of the EG layers. These changes reduced the electrical properties of the EG.

Destruction of chloroform

Figure 5a shows the efficiency of chloroform decomposition in DBD reactor (the error was less than ±3.4 %). The results showed that it increased by increasing voltage from 15 to 20 kV. In addition, other studies have reported that the efficiency increases when there is an increase in applied voltage which is because of active species and collision increase with pollutant resulting in an increase in removal efficiency (Kwong et al. 2008; Liang et al. 2013; Mista and Kacprzyk 2008; Oh et al. 2009). In NTP process, linear decrease in removal of dichloromethane and benzene has been reported by increasing inlet concentration (Abd Allah et al. 2013; Karuppiah et al. 2012a, b, c). Inlet concentration increase requires more active species for degradation (Abd Allah et al. 2013). The findings of this study showed that removal efficiency enhanced by increasing the inlet concentration (Fig. 5a). The removal efficiency at concentration of 85 ppm, flow rate of 0.3 L/min and applied voltage of 20 kV was 70 %, which went up by 4 and 6 %, respectively, for concentrations of 250 and 500 ppm.

Removal efficiency difference between this study and other works could be owing to the applied reactor; in this study because of using the EG as discharge electrode, the distance between the discharge electrode and ground was 15 mm, and in view of the fact that the EG was porous, the discharge gape can be considered 20 mm. In comparison with past studies, the discharge gape was very larger (Agnihotri et al. 2004; Guaitella et al. 2006; Karuppiah et al. 2012a, b, c). Thus, in view of being larger the area of electrical discharge, at low concentrations, the probability of collision between the generated active species and pollutant molecules is low which increases by increasing concentration and then the efficiency goes up. Further studies are needed to deal with possible disadvantages of this new reactor such as graphite oxidation at high temperature or reduction in electrical field power.

In this study, the effect of flow rate on the removal efficiency was also investigated. Figure 5a shows chloroform removal efficiency at the flow rates of 0.3, 0.6 and 1.2 L/min that correspond to residence times of 2, 1 and 0.5 s, respectively. By increasing the flow rate from 0.3 to 0.6 and 1.2 L/min, at applied voltage of 15 kV, on the average 16 and 19 % decrease in efficiency, respectively,

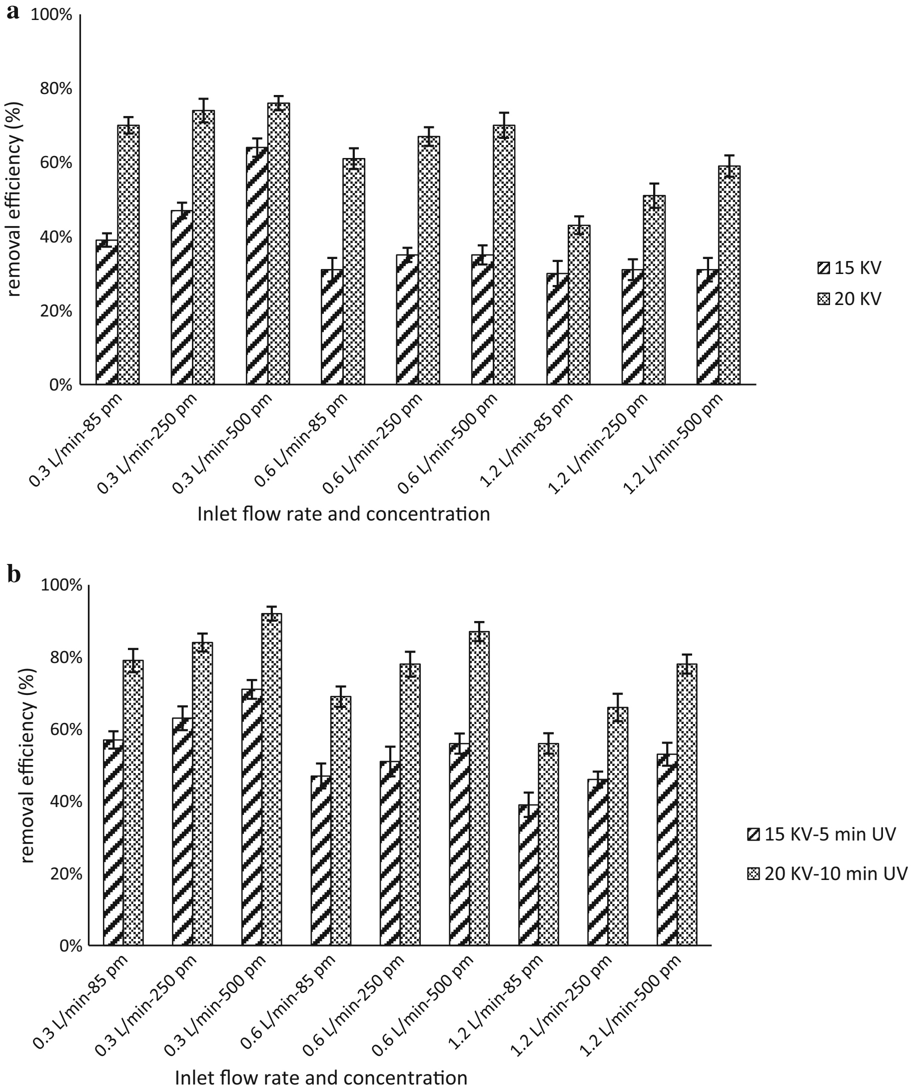

Fig. 5 Chloroform decomposition: **a** NTP system, **b** hybrid system

was seen; and, at applied voltage of 20 kV, respectively, the efficiency decreased by 7 and 22 %. Abd Allah et al. (2013) illustrated that increased residence time raised chlorinated VOC removal efficiency in plasma process. An increase in residence time of gas components in plasma leads to the formation of more active species in unit volume of plasma.

Figure 5b shows chloroform removal efficiency in NTP–PCO system (the error was less than ±3.4 %). Comparison of Fig. 5a and b shows that more increase in efficiency (22 %) took place at the applied voltage of 15 kV and ultraviolet irradiation of 5 min. In view of the fact that low applied voltage and UV irradiation time resulted in a decrease in generation of active species for oxidation in NTP and PCO processes, this removal efficiency increase was because of the fact that at the voltage of 20 kV much concentration of chloroform was decomposed in NTP and lower content of the pollutant was transformed to the PCO process. Best performance of photocatalysis process is usually at high concentrations of pollutant (Lu et al. 2012).

By-products

The application of NTP for VOCs abatement suffers from many weaknesses, i.e., incomplete oxidation with emission of harmful by-products such as O_3 and NO_x (Vandenbroucke et al. 2011). The NTP process breaks down oxygen molecules into oxygen radicals; the oxygen radicals combine with oxygen molecules to create ozone as described in Eqs. (1) and (2) (Abedi et al. 2015; Kwong et al. 2008; Liang et al. 2013; Mista and Kacprzyk 2008).

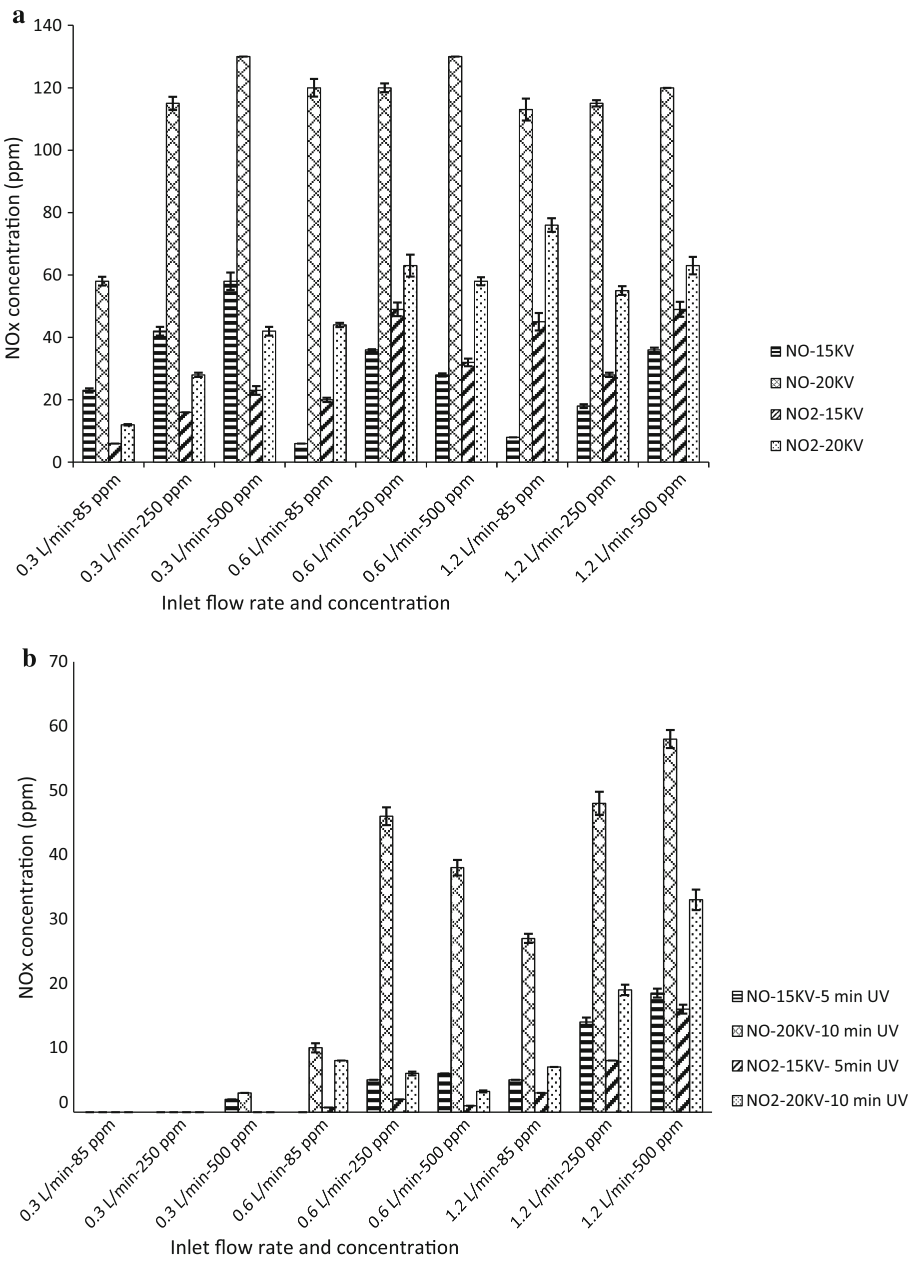

Fig. 6 Concentration of produced NO_x: **a** NTP system, **b** hybrid system

$$\mathrm{e} + \mathrm{O}_2 \rightarrow \mathrm{e} + \mathrm{O}^{\cdot} + \mathrm{O}^{\cdot} \tag{1}$$

$$\mathrm{O}^{\cdot} + \mathrm{O}_2 + \mathrm{M} \rightarrow \mathrm{O}_3 + \mathrm{M} \tag{2}$$

M component is needed to absorb the extra energy. In the case of air, this component is oxygen or nitrogen molecules (Liang et al. 2013).

The amount of the generated ozone from the NTP process was low (about 40–42 ppm). This low amount of ozone can be attributed to the applied voltage and porous structure of the discharge electrode. Ozone has a very strong oxidizing capability; in the presence of ozone, zeolite and many porous materials may act as a catalyst owing to ion exchange and other chemical features, which consequently degrade ozone to atomic and molecular oxygen (Kwong et al. 2008). At voltages above 15 kV due to generation of excess high-energy electrons, the created ozone is decomposed by collision to these excess high-energy electrons and generates radical and molecular oxygen and hence the ozone concentration falls (Liang et al. 2013).

When PCO was added downstream the NTP system, there were various advanced oxidation processes (AOPs) including UV/TiO_2, O_3/UV and O_3/TiO_2. Ozone, unwanted

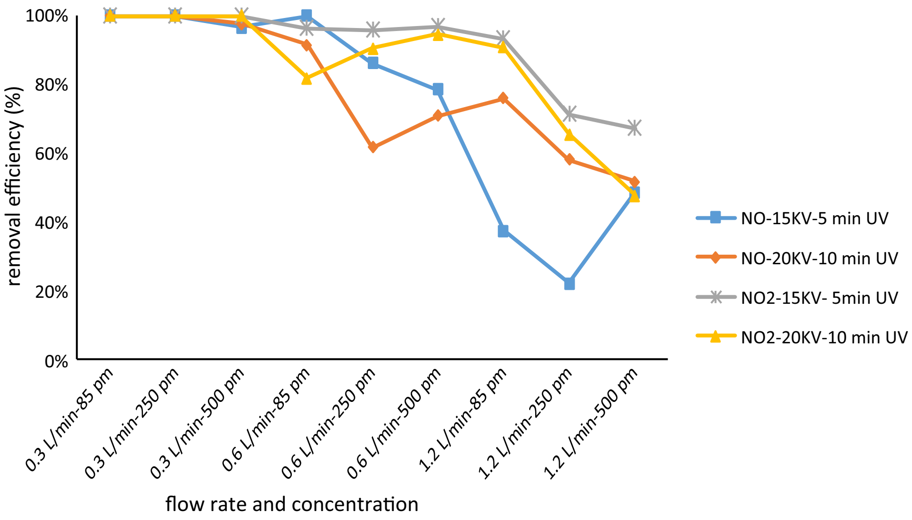

Fig. 7 Degradation of produced NO_x in DBD reactor by hybrid system

by-product of plasma, is a strong oxidant agent. It is utilized as the oxidant precursor by PCO and improved removal efficiency and durability of photocatalyst (Huang and Ye 2009). In PCO process, ozone is decomposed to atomic and molecular oxygen by UV irradiation or catalyst as Eq. (3).

$$O_3 \xrightarrow{\text{hvorcatalyst}} O_2 + O^{\cdot} \quad (3)$$

In this study, this low amount of the produced ozone in NTP process was degraded in PCO by TiO_2 and ZnO catalysts as well as UV radiation, so that in the output of the NTP–PCO system ozone was not detected.

In NTP, the generation of NO is inevitable in the presence of O_2 and N_2; NO can be easily oxidized to NO_2 by proxy radicals or ozone (Oh et al. 2009). The generation of NO and its conversion to NO_2 can be written as Eqs. (4–7) (Pekárek 2003).

$$e + N_2 \rightarrow N^{\cdot} + N^{\cdot} + e \quad (4)$$

$$N^{\cdot} + O_2 \rightarrow NO + O^{\cdot} \quad (5)$$

$$N^{\cdot} + O_3 \rightarrow NO + O_2 \quad (6)$$

$$NO + O_3 \rightarrow NO_2 + O_2 \quad (7)$$

Figure 6a shows the created NO and NO_2 in NTP process (the error was less than ±5.2 %). As can be seen, it was as a function of applied voltage and flow rate; the concentrations of NO and NO_2 increased by increasing the applied voltage. This increase can be attributed to increase in the number of free electrons resulting in collision increase and creation of NO and NO_2.

Photo-decomposition, photo-oxidation and photo-selective catalytic reduction (photo-SCR) are methods that have been presented for photocatalytic degradation of NO_x in literature. The photo-decomposition process occurs via reaction on the photocatalyst surface and it is focused on increasing the toward N_2 production. In Photo-selective catalytic reduction (photo-SCR) method, NO_x reduction happens in the presence of a reducing agent such as NH_3 or hydrocarbons under light irradiation. This process occurs on a photocatalyst surface and transfers NO_x into harmless gaseous compounds, such as N_2. The aim of photo-oxidation is to transform NO into HNO_3 through the formation of HNO_2 and NO_2 (Maggos et al. 2007).

Figure 6b shows the output amount of NO and NO_2 from the NTP–PCO system (the error was less than ±4.8 %). As can be clearly seen, high concentrations of the produced NO and NO_2 in NTP process were removed by PCO (Fig. 6a, b). NO_x removal efficiency in PCO process was a function of flow rate and initial concentration.

The efficiency was 100 % at the flow rate of 0.3 L/min; by increasing the flow rate, it decreased to 22 % at the flow rate of 1.2 L/min (Fig. 7). This decrease in efficiency was owing to residence time decrease in reactor as well as space velocity increase of pollutants. At lower flow rates, the residence time of NO_x in the reactor was higher, so the collision probability of NO_x with the active species was higher and therefore the removal efficiency was higher. Moreover, increase in inlet concentration led to saturation of the catalyst active sites and hence reduced removal efficiency. Devahasdin et al. (2003) reported that NO_x removal efficiency increased with increasing residence time and decreasing inlet concentration.

In any case of the all experiments, a sample was injected to GC–MS for by-product detection; the results showed that the output gas from the NTP process contained chloroform, phosgene, trichloroacetaldehyde, chlorine and carbon dioxide (Fig. 8a). In view of high probability of HCl creation and lack of its detection by GC–MS, the

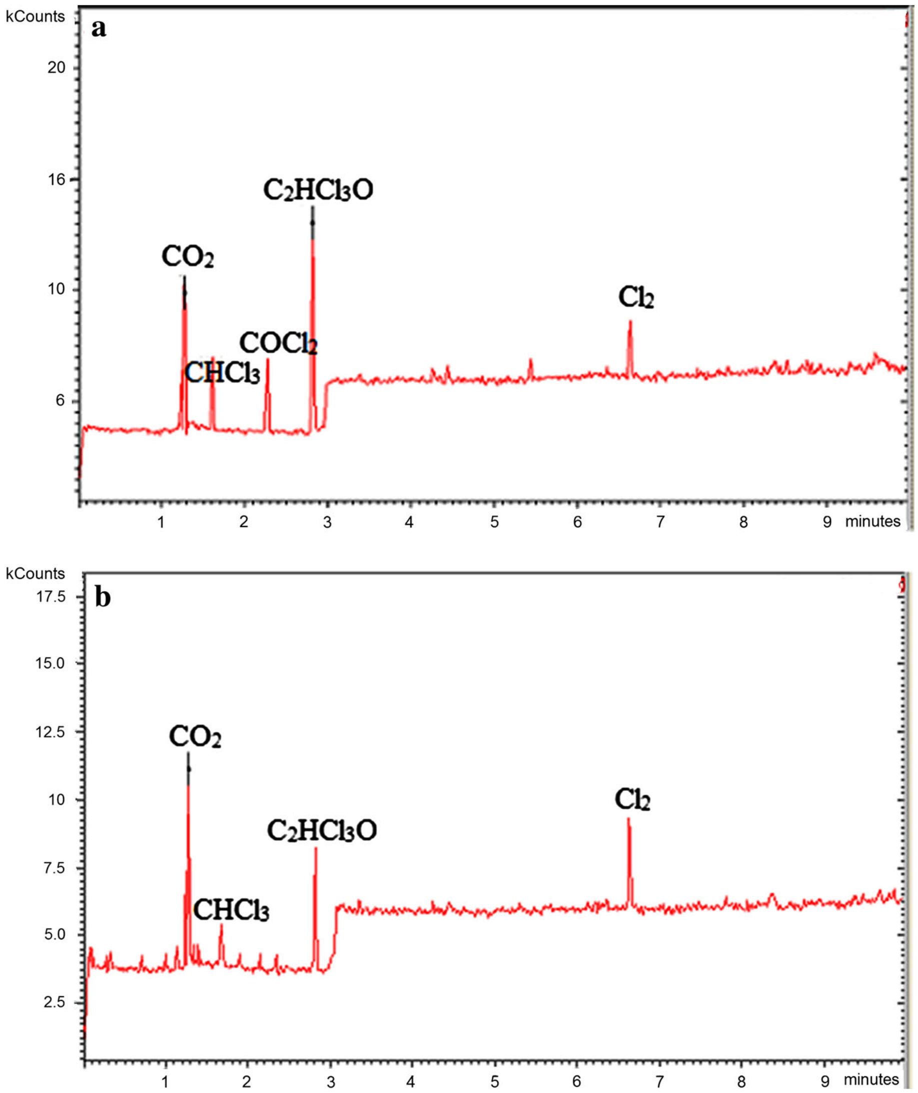

Fig. 8 GC–MS chromatogram: **a** GC–MS chromatogram for non-thermal plasma process, **b** GC–MS chromatogram for combined process

output gas was analyzed by HCl detector tube and showed this compound was created by chloroform degradation.

The most probably and commonly accepted pathway for degradation of VOCs in NTP process is collision pathway, in which high-energy electrons contact with elements existing in the gas flow and create active radicals, ions and species which are oxide VOCs (Kalpathi 2005). Regarding the ingredient of the input gas to the plasma reactor, some of reactions of electron collision may be written as follows:

$$\mathrm{e} + \mathrm{O_2} \rightarrow \mathrm{e} + \mathrm{O}^{\cdot} + \mathrm{O}^{\cdot} \tag{8}$$

$$\mathrm{e} + \mathrm{H_2O} \rightarrow \mathrm{H}^{-} + \mathrm{OH}^{\cdot} \tag{9}$$

$$\mathrm{e} + \mathrm{CHCl_3} \rightarrow \mathrm{CHCl_2} + \mathrm{Cl}^{\cdot} \tag{10}$$

In view of the presence of radicals of oxygen and chlorine, a few pathways of chloroform destruction can be written as follows (Bakar et al. 2010; Főglein et al. 2005; Indarto et al. 2006):

$$\mathrm{CHCl_3} + \mathrm{O}^{\cdot} \rightarrow \mathrm{COCl_2} + \mathrm{HCl} \tag{11}$$

$$\mathrm{COCl_2} + \mathrm{O}^{\cdot} \rightarrow \mathrm{CO_2} + \mathrm{Cl_2} \tag{12}$$

$$\mathrm{COCl_2} + \mathrm{Cl}^{\cdot} \rightarrow \mathrm{COCl}^{\cdot} + \mathrm{Cl_2} \tag{13}$$

$$\mathrm{COCl}^{\cdot} + \mathrm{CHCl_3} \rightarrow \mathrm{CHCOCl}_2^{\cdot} \tag{14}$$

$$\mathrm{CHCOCl}_2^{\cdot} + \mathrm{Cl}^{\cdot} \rightarrow \mathrm{C_2HCl_3O} \tag{15}$$

$$\mathrm{CHCl_3} + \mathrm{Cl}^{\cdot} \rightarrow \mathrm{CCl_3} + \mathrm{HCl} \tag{16}$$

Comparison of Fig. 8a and b shows that most part of the created organic by-products in plasma reactor were oxidized in combined system and their concentration decreased in the effluent. For example, phosgene, one of the generated by-products in plasma reactor, is formed because of the reaction between chloroform and atomic or radical oxygen (Eq. 11). Phosgene has high toxicity which is not acceptable in effluent. In combined system, because of the created ozone and additional oxidation process: ozone/photocatalysis and catalytic ozonation, there are more active radicals such as proxy, hydroxyl and chlorine, which can convert phosgene to low-toxic products like CO_2 and Cl_2 (Eqs. 17–20) (Bakar et al. 2010; Lee et al. 1996).

$$\mathrm{COCl_2} + h\nu \rightarrow \mathrm{CO} + 2\mathrm{Cl}^{\cdot} \tag{17}$$

$$\mathrm{COCl_2} + \mathrm{Cl}^{\cdot} \rightarrow \mathrm{COCl}^{\cdot} + \mathrm{Cl_2} \tag{18}$$

$$\mathrm{COCl_2} + \mathrm{H}^{\cdot} \rightarrow \mathrm{COCl}^{\cdot} + \mathrm{HCl} \tag{19}$$

$$\mathrm{COCl_2} + \mathrm{O}^{\cdot} \rightarrow \mathrm{CO_2} + \mathrm{Cl_2} \tag{20}$$

Similar to phosgene, trichloroacetaldehyde is also oxidized in combined system; following pathways for photocatalytic destruction of trichloroacetaldehyde have been reported (Driessen et al. 1998; Fan and Yates 1996).

$$\begin{aligned}\mathrm{C_2HCl_3O} + \mathrm{O_2^{\cdot}} \rightarrow\ & \mathrm{COCl_2} + \mathrm{CO} + \mathrm{CO_2} + \mathrm{HCl} \\ & + \mathrm{CHCl_3}(\mathrm{trace})\end{aligned} \tag{21}$$

$$\mathrm{C_2HCl_3O} + \frac{1}{2}\mathrm{O_2} \rightarrow \mathrm{COCl_2} + \mathrm{HCl} + \mathrm{CO} \tag{22}$$

Besides oxidation of the created organic by-products, un-oxidized chloroform is reoxidized in combined system (Eqs. 23–27) (Bakar et al. 2010).

$$\mathrm{CHCl_3} + h\nu \rightarrow \mathrm{CHCl_2} + \mathrm{Cl}^{\cdot} \tag{23}$$

$$\mathrm{CHCl_2} + \mathrm{OH}^{\cdot} \rightarrow \mathrm{CH_2Cl} + \mathrm{OCl} \tag{24}$$

$$\mathrm{CH_2Cl} + \mathrm{H}^{\cdot} \rightarrow \mathrm{CH_3Cl} \tag{25}$$

$$\mathrm{CHCl_3} + \mathrm{OH}^{\cdot} \rightarrow \mathrm{H_2O} + \mathrm{CCl_3} \tag{26}$$

$$\mathrm{CHCl_3} + \mathrm{Cl}^{\cdot} \rightarrow \mathrm{CCl_3} + \mathrm{HCl} \tag{27}$$

As can be clearly seen in Fig. 8a, b, reoxidation of the generated organic by-products in combined system decreased their contents and increased the selectivity of CO_2 and Cl_2.

Conclusion

In this study, the decomposition of chloroform vapors in a NTP reactor as well as a combined system of this reactor in conjunction with photocatalyst was investigated. The findings showed that the efficiency decreased by increasing flow rate, which was because of the fact that residence time decreased. However, by increasing the inlet concentration in NTP system higher efficiency was seen, because the reactor had larger discharge gap. Analysis of the output gas showed that the NTP system had high concentration of NO and NO_2, but in combined system the concentration of these two pollutants dropped dramatically. NO_x removal efficiency for the PCO system was a function of flow rate and it increased when flow rate increased. The content of effluent ozone from the DBD reactor was little and constant which might be on account of the EG in the reactor, which acted as a catalyst in the presence of ozone and degraded ozone. The generated ozone from the NTP system was degraded in PCO and consequently was not detected in output gas of the combined system. The generated organic by-products in NTP process were: phosgene and trichloroacetaldehyde, which were reoxidized with un-oxidized chloroform in the second stage of the combined system. This increased the selectivity of CO_2 and Cl_2. Based on these results, the combined system is preferred due to higher removal efficiency, complete mineralization and lower harmful by-products.

Acknowledgments Authors would like to thank Hamadan University of Medical Sciences for the financial support under PhD thesis scheme (Grant Number: 9204181276). In addition, thanks Dr. Godini Kazem for the help.

References

Abd Allah Z, Whitehead JC, Martin P (2013) Remediation of dichloromethane (CH_2Cl_2) using non-thermal, atmospheric pressure plasma generated in a packed-bed reactor. Environ Sci Technol 48(1):558–565. doi:10.1021/es402953z

Abedi K, Ghorbani-Shahna F, Jaleh B, Bahrami A, Mousavi S, Haddadi R, Gandomi M (2015) Decomposition of chlorinated volatile organic compounds (CVOCs) using NTP coupled with TiO_2/GAC, ZnO/GAC, and TiO_2–ZnO/GAC in a plasma-assisted catalysis system. J Electrostat 73:80–88. doi:10.1016/j.elstat.2014.10.008

Agnihotri S, Cal MP, Prien J (2004) Destruction of 1,1,1-trichloroethane using dielectric barrier discharge nonthermal plasma. J Environ Eng 130(3):349–355. doi:10.1061/(ASCE)0733-9372(2004)130:3(349)

Bakar W, Ali R, Othman M (2010) Photocatalytic degradation and reaction pathway studies of chlorinated hydrocarbons in gaseous phase. Trans C Chem Chem Eng 17(1):1–14

Devahasdin S, Fan C, Li K, Chen DH (2003) TiO_2 photocatalytic oxidation of nitric oxide: transient behavior and reaction kinetics. J Photochem Photobiol A 156(1):161–170. doi:10.1016/S1010-6030(03)00005-4

Driessen M, Goodman A, Miller T, Zaharias G, Grassian V (1998) Gas-phase photooxidation of trichloroethylene on TiO_2 and ZnO: influence of trichloroethylene pressure, oxygen pressure, and the photocatalyst surface on the product distribution. J Phys Chem B 102(3):549–556. doi:10.1021/jp972351e

Fan J, Yates JT (1996) Mechanism of photooxidation of trichloroethylene on TiO_2: detection of intermediates by infrared spectroscopy. J Am Chem Soc 118(19):4686–4692. doi:10.1021/ja952155q

Főglein KA, Szépvölgyi J, Szabó PT, Mészáros E, Pekker-Jakab E, Babievskaya IZ, Mohai I, Károly Z (2005) Comparative study on decomposition of $CFCl_3$ in thermal and cold plasma. Plasma Chem Plasma Process 25(3):275–288. doi:10.1007/s11090-004-3040-z

Guaitella O, Thevenet F, Guillard C, Rousseau A (2006) Dynamic of the plasma current amplitude in a barrier discharge: influence of photocatalytic material. J Phys D Appl Phys 39(14):2964–2972. doi:10.1088/0022-3727/39/14/015

Huang H, Ye D (2009) Combination of photocatalysis downstream the non-thermal plasma reactor for oxidation of gas-phase toluene. J Hazard Mater 171(1):535–541. doi:10.1016/j.jhazmat.2009.06.033

Indarto A, Choi JW, Lee H, Hk Song (2006) Decomposition of CCl_4 and $CHCl_3$ on gliding arc plasma. J Environ Sci 18(1):83–89

Kalpathi V (2005). Destruction of volatile organic compounds in a dielectric barrier discharge plasma reactor. Ph.D. Dissertation, Oklahoma State University, USA

Karuppiah J, Reddy EL, Sivachandiran L, Karvembu R, Subrahmanyam C (2012a) Nonthermal plasma assisted photocatalytic oxidation of dilute benzene. J Chem Sci 124(4):841–845. doi:10.1007/s12039-012-0282-9

Karuppiah J, Linga Reddy E, Manoj Kumar Reddy P, Ramaraju B, Karvembu R, Subrahmanyam C (2012b) Abatement of mixture of volatile organic compounds (VOCs) in a catalytic non-thermal plasma reactor. J Hazard Mater 237:283–289. doi:10.1016/j.jhazmat.2012.08.040

Karuppiah J, Karvembu R, Subrahmanyam C (2012c) The catalytic effect of MnO_x and CoO_x on the decomposition of nitrobenzene in a non-thermal plasma reactor. Chem Eng J 180:39–45. doi:10.1016/j.cej.2011.10.096

Kwong CW, Chao CY, Hui K, Wan M (2008) Removal of VOCs from indoor environment by ozonation over different porous materials. Atmos Environ 42(10):2300–2311. doi:10.1016/j.atmosenv.2007.12.030

Lee WJ, Chen CY, Lin WC, Wang YT, Chin CJ (1996) Phosgene formation from the decomposition of 1,1-$C_2H_2Cl_2$ contained gas in an RF plasma reactor. J Hazard Mater 48(1):51–67. doi:10.1016/0304-3894(95)00145-X

Liang WJ, Ma L, Liu H, Li J (2013) Toluene degradation by non-thermal plasma combined with a ferroelectric catalyst. Chemosphere 92(10):1390–1395. doi:10.1016/j.chemosphere.2013.05.042

Lu Y, Wang D, Wu Y, Ma C, Zhang X, Yang C (2012) Synergistic effect of nanophotocatalysis and nonthermal plasma on the removal of indoor HCHO. Int J Photoenergy 2012:1–8. doi:10.1155/2012/354032

Maciuca A, Batiot-Dupeyrat C, Tatibouët JM (2012) Synergetic effect by coupling photocatalysis with plasma for low VOCs concentration removal from air. Appl Catal B 125:432–438. doi:10.1016/j.apcatb.2012.06.012

Maggos T, Bartzis J, Leva P, Kotzias D (2007) Application of photocatalytic technology for NO_x removal. Appl Phys A 89(1):81–84. doi:10.1007/s00339-007-4033-6

Magureanu M, Mandache N, Parvulescu V (2007) Chlorinated organic compounds decomposition in a dielectric barrier discharge. Plasma Chem Plasma Process 27(6):679–690. doi:10.1007/s11090-007-9103-1

Mista W, Kacprzyk R (2008) Decomposition of toluene using non-thermal plasma reactor at room temperature. Catal Today 137(2):345–349. doi:10.1016/j.cattod.2008.02.009

Oh J-H, Mok YS, Lee S-B, Chang MS (2009) Destruction of HCFC-22 and distribution of byproducts in a nonthermal plasma reactor packed with dielectric pellets. J Korean Phys Soc 54(4):1539–1546. doi:10.3938/jkps.54.1539

Pal B, Sharon M (2002) Enhanced photocatalytic activity of highly porous ZnO thin films prepared by sol–gel process. Mater Chem Phys 76(1):82–87. doi:10.1016/S0254-0584(01)00514-4

Pekárek S (2003) Non-thermal plasma ozone generation. Acta Polytech 43(6):47–51

Subrahmanyam C, Magureanu M, Renken A, Kiwi-Minsker L (2006) Catalytic abatement of volatile organic compounds assisted by non-thermal plasma: Part 1. A novel dielectric barrier discharge reactor containing catalytic electrode. Appl Catal B 65(1):150–156. doi:10.1016/j.apcatb.2006.01.006

Subrahmanyam C, Renken A, Kiwi-Minsker L (2007a) Novel catalytic non-thermal plasma reactor for the abatement of VOCs. Chem Eng J 134(1):78–83. doi:10.1016/j.cej.2007.03.063

Subrahmanyam C, Magureanu M, Laub D, Renken A, Kiwi-Minsker L (2007b) Nonthermal plasma abatement of trichloroethylene enhanced by photocatalysis. J Phys Chem C 111(11):4315–4318. doi:10.1021/jp066731o

Sun R-B, Xi Z-G, Chao F-H, Zhang W, Zhang H-S, Yang D-F (2007) Decomposition of low-concentration gas-phase toluene using plasma-driven photocatalyst reactor. Atmos Environ 41(32):6853–6859. doi:10.1016/j.atmosenv.2007.04.041

Thevenet F, Guaitella O, Puzenat E, Herrmann J-M, Rousseau A, Guillard C (2007) Oxidation of acetylene by photocatalysis coupled with dielectric barrier discharge. Catal Today 122(1):186–194. doi:10.1016/j.cattod.2007.01.057

Vandenbroucke AM, Morent R, De Geyter N, Leys C (2011) Non-thermal plasmas for non-catalytic and catalytic VOC abatement. J Hazard Mater 195:30–54. doi:10.1016/j.jhazmat.2011.08.060

Yan H, Chunwei Y (2006) Low-temperature preparation of photocatalytic TiO_2 thin films on polymer substrates by direct deposition from anatase sol. J Mater Sci Technol 22(2):239–244

Zhu T, Li J, Y-q Jin, Liang Y, Ma G (2008) Decomposition of benzene by non-thermal plasma processing: photocatalyst and ozone effect. Int J Sci Technol 5(3):375–384